

Exploring the expression of SNHG1 and its effect on the PI3K-AKT axis in nasopharyngeal cancer

Yong YANG^{1,2}, Yan-Ping YANG¹, Mei-Ling YI¹, Fang-Ting HUANG², Xia ZHU², Guang-Wu HUANG^{1,*}

¹Department of Otolaryngology-Head and Neck Surgery, The First Affiliated Hospital of Guangxi Medical University, Nanning, China; ²Department of Otolaryngology-Head and Neck Surgery, The First People's Hospital of Nanning, Nanning, China

*Correspondence: hgw1288@126.com

Received May 17, 2023 / Accepted October 27, 2023

Radiotherapy and chemotherapy have improved the 5-year survival rate of nasopharyngeal carcinoma (NPC) patients, but the side effects generally lead to unsatisfactory clinical efficacy. It's imperative to explore the pathogenesis of NPC to find better diagnostic and therapeutic methods. Small nucleolar RNA host genes (SNHG1) are special lncRNAs, which can be further spliced to produce small nucleolar RNAs (snoRNAs). SNHG1 has been found to be associated with various cancers. However, only a few studies reported the relationship between SNHG1 and NPC. This study first analyzed the diagnostic performance and related signaling pathways of SNHG1 in NPC through bioinformatics. The expression of SNHG1 was verified by RT-qPCR, and the expression of the signaling pathway was detected using immunohistochemistry. Bioinformatics analysis results showed that SNHG1 was significantly overexpressed in head and neck squamous cell carcinoma (HNSC) and NPC tissues. RT-qPCR detection confirmed the significant overexpression of SNHG1 in NPC tissues. Enrichment analysis showed that SNHG1 may act on NPC through the PI3K-AKT signaling pathway. Immunohistochemistry experiment revealed PI3K-AKT signaling pathway proteins (PI3K AKT and EGFR) positively expressed and CASP3 weakly positively expressed in NPC tissues. Therefore, we concluded that SNHG1 is a prospective biomarker and may act on NPC through the PI3K-AKT signaling pathway.

Key words: nasopharyngeal carcinoma; SNHG1; PI3K-AKT

Nasopharyngeal carcinoma (NPC) is an epithelial malignant tumor with the highest metastatic potential among head and neck cancers [1, 2]. In terms of treatment, radiotherapy combined with chemotherapy can help improve the survival time of patients with NPC. However, about 30% of patients with NPC still have a poor prognosis, mainly due to the fact that some patients have advanced stage and distant metastasis at the time of diagnosis [3]. The combination of cisplatin and 5-fluorouracil is currently the first-line treatment for recurrent or metastatic diseases but the remission rate is only 40–65% [4]. The high expression of PD-L1 in NPC may make patients suitable for immune checkpoint-blocking therapy but PD-1 inhibitors are only beneficial to some patients [5]. Therefore, it's necessary to further explore the pathogenesis of NPC, and explore biomarkers related to prognostic risk stratification and treatment benefits to optimize treatment strategies for different patient subsets. Studies have shown that lncRNA is involved in malignant phenotypes such as carcinogenesis, migration, invasion, epithelial-mesenchymal

transformation (EMT), and angiogenesis in NPC [6]. It is an important biomarker for the diagnosis and prognosis of NPC and mediates radio-chemotherapy resistance in multiple ways [7].

Small nucleolar RNA (snoRNA) is widely found in the nucleoli of eukaryotic cells, with a length of 60–300 nt, and can bind to ribonucleoproteins to form snoRNPs complexes [8]. Small nucleolar RNA host genes (SNHG1) are a class of special lncRNAs that can be further spliced to produce snoRNA. The member of the SNHG1 family, SNHG1, is formed by transcription of the U22 host gene on chromosome 11. It has a total length of approximately 3,927 bases and contains 9 snoRNAs [9, 10]. SNHG1 has been confirmed to play a role as a tumor-promoting factor in various malignant tumors, which can inhibit the expression of the p53 gene and promote tumor cell proliferation, invasion, and metastasis [11]. Zhou et al. found that SNHG1 could promote NPC development by inhibiting the expression of miR-424-5p [12]. However, there is still a lack of theoretical



basis for analyzing the mechanism of SNHG1 in NPC, and further research is needed to explore its clinical value in the prevention, diagnosis, treatment, and prognosis of NPC.

Therefore, this study was based on bioinformatics and experimental methods, using TCGA and GEO expression profile data to study the expression of SNHG1 in head and neck squamous carcinoma (HNSC) and NPC. RT-qPCR was conducted to verify the expression of SNHG1 in NPC tissue, as well as an immunohistochemical experiment to explore the possible new targets and related signaling pathways for NPC.

Patients and methods

Materials. We collected 4 pairs of fresh NPC and adjacent non-cancerous tissues, as well as 36 nasopharyngitis (NPS) and 36 NPC tissue wax blocks. All samples originated from the nasopharynx with the approval of the Ethics Committee of the First Affiliated Hospital of Guangxi Medical University (No.2021-KY-E-208) and the informed consent of patients. Antibodies used in this study included rabbit anti-human monoclonal antibody PI3K (ab151549, 1:100), rabbit anti-human monoclonal antibody AKT (ab179463, 1:200), horseradish peroxidase-labeled goat-derived anti-rabbit IgG antibodies (ab6721, 1:500) and horseradish peroxidase-labeled goat-derived anti-mouse IgG antibodies (ab97240, 1:500) (Abcam, USA); mouse anti-human monoclonal antibody p-AKT (664441-g, 1:100) (Proteintech, China); rabbit anti-human monoclonal antibody EGFR (AF6043, 1:100), and rabbit anti-human monoclonal antibody Caspase 3 (CASP3) (AF6311, 1:100) (Affinity, USA).

Expression analysis of SNHG1 in NPC. The Tumor Immune Estimation Resource (TIMER, <http://timer.cistrome.org/>) and Gene Expression Profiling Interactive Analysis 2 (GEPIA2, <http://gepia2.cancer-pku.cn/#index>) databases were used to analyze the differential expression of SNHG1 in HNSC and adjacent tissues. Box charts were used to display the distribution of gene expression levels. The NPC datasets GSE61218 and GSE53819 were downloaded from the NCBI GEO database (<https://www.ncbi.nlm.nih.gov/geo/>). The R language “limma” package was conducted to perform a non-paired t-test on the SNHG1 expression in NPC based on the GEO dataset. We used the beeswarm package to draw a honey map for visualization and calculated a statistical significance using the Wilcoxon test function test. Based on the University of Alabama at Birmingham Cancer Data Analysis Portal (UALCAN, <http://ualcan.path.uab.edu/>) database, we analyzed the expression level of SNHG1 in HNSC under different clinical characteristics, including the presence or absence of HPV virus and so on (* $p < 0.05$, ** $p < 0.01$, *** $p < 0.001$).

Diagnostic performance of SNHG1 for NPC. According to NPC samples in the GEO database, the receiver operating characteristic (ROC) curve was drawn using the R language pROC package and ggplot2 function. ROC could deter-

mine the diagnostic performance of SNHG1 in NPC. The area under the curve (AUC) is between 1.0 and 0.5. When $AUC > 0.5$, the closer the AUC is to 1, the better the diagnostic effect. AUC has a low accuracy at 0.5–0.7, a certain accuracy at 0.7–0.9, and a higher accuracy at above 0.9. When $AUC = 0.5$, it indicates that the diagnostic method is completely ineffective and has no diagnostic value.

SNHG1 immune correlation analysis. Tumor immune microenvironment is closely related to factors such as inflammatory factor expression, immune cell infiltration, microvascular invasion, chromosome instability, and TP53 mutation. In this study, the TIMER2.0 database was used to analyze the correlation between SNHG1 and immune cell infiltration in HNSC, with a statistically significant difference of $p < 0.05$.

Analysis of SNHG1 differentially expressed genes (DEGs). The NPC samples were grouped according to the expression of SNHG1 in GEO datasets. The R language “limma” package was used to perform DEGs analysis. The DEGs were screened using the gene expression multiple change $|\log_2FC| > 1$, and $p < 0.05$ as the criteria. The R language plot function was used to draw a volcanic map and a heat map.

Protein-Protein Interaction Networks (PPI). We imported the DEGs of SNHG1 into the STRING database (<https://string-db.org>), selected “multiple protocols”, then defined the attribution as “Homo sapiens”, and hid the free nodes. Other parameters were kept at default values to obtain the intersection target interaction network. At the same time, we set the data with a medium confidence > 0.4 to ensure the reliability of this analysis. We downloaded tsv format file and established a corresponding relationship between the selected protein nodes. Cytoscape 3.9.1 software was performed for visualization, the cytoHubba plug-in for sorting core target genes by Degree, and the MCODE plug-in of Cytoscape for constructing a subnetwork.

Gene function enrichment analysis. Gene Ontology (GO) analysis includes cell components (CC), molecular function (MF), and biological process (BP) analysis. Kyoto Encyclopedia of Genes and Genomes (KEGG) analysis integrates genomic, chemical, and system functional information. We used DEGs of SNHG1 as the gene set for enrichment analysis, and the R language org.Hs.eg.db package was conducted to obtain the entrezID corresponding to the candidate genes. The cluster profiler package was performed to carry out GO and KEGG enrichment analysis with point maps respectively.

RT-qPCR. Four pairs of fresh NPC and adjacent non-cancerous tissues were used for RT-qPCR detection. Total RNA was extracted with a TRIzol kit, and cDNA was synthesized using reverse transcriptase before PCR amplification. Reaction conditions: a two-step reaction procedure was set up. PCR reaction (40 cycles): pre-denaturation at 95°C for 30 s; chain breaking at 95°C for 3 s; annealing, and extension at 60°C for 30 s. Melt curve: use the instrument default program. After the reaction was completed, data such as Ct

values were derived, and statistical analysis was performed using the $2^{-\Delta\Delta CT}$ method. The primers used in this study were all purchased from SANGON BIOTECH (Shanghai). Inc SNHG1: CAGCACCTTCTCTAAAGCCCAAG (forward), TCAGACCTGAACTTCAGACCTGGAG (reverse). Reference GAPDH: GACAGTCAGCGCGCATCTTCT (forward), GCGCCAATACCACAATC (reverse).

Hematoxylin-Eosin (H&E) staining for histopathological analysis. The paraffin slices were subjected to de-waxing with xylene and hydration with gradient ethanol, each lasting for 5 min. The slides were thoroughly washed prior to staining with hematoxylin dye solution for 10 min, followed by rinsing with running water. To remove excess stain, the slides were treated with 1% hydrochloric acid ethanol and washed with double-distilled water. The subsequent weak alkaline blue promoter solution and eosin staining lasted for 3 min. Gradual dehydration was performed using gradient ethanol, with each concentration maintained for 2 min. Finally, the slides were treated with xylene, sealed with neutral gum, and observed under a microscope to capture images.

Immunohistochemical (IHC) detection. 3% H_2O_2 was used to inhibit the endogenous peroxidase activity in the slices. 4% of normal goat serum was added for blocking.

Antibodies (PI3K, AKT, p-AKT, EGFR, and CASP3) were added and incubated overnight at 4°C. After that, the slices were incubated with the second antibody at 37°C for 1 h. Hematoxylin staining was performed for microscopic observation.

Results

Expression of SNHG1 in NPC. Compared with non-cancerous tissues, SNHG1 is significantly overexpressed in HNSC tissues both in the TIMER2.0 ($p < 0.05$, Figure 1A) and GEPIA2 ($p < 0.05$, Figure 1B) databases. SNHG1 significantly differentially expressed in pan-cancer tissues is shown in Supplementary Figure S1 ($p < 0.05$). We further analyzed the expression of SNHG1 in NPC through the GEO database (GSE61218 and GSE53819). Compared with non-cancerous tissues, SNHG1 is significantly overexpressed in NPC tissues ($p < 0.05$, Figures 1C, 1D). We used RT-qPCR to detect the transcriptional level of SNHG1 in 4 pairs of fresh NPC and adjacent non-cancerous tissues. Compared with the adjacent non-cancerous tissues, the transcription level of SNHG1 in NPC tissues is significantly upregulated ($p < 0.05$, Figure 1E). The RT-qPCR results are consistent with the bioinformatics

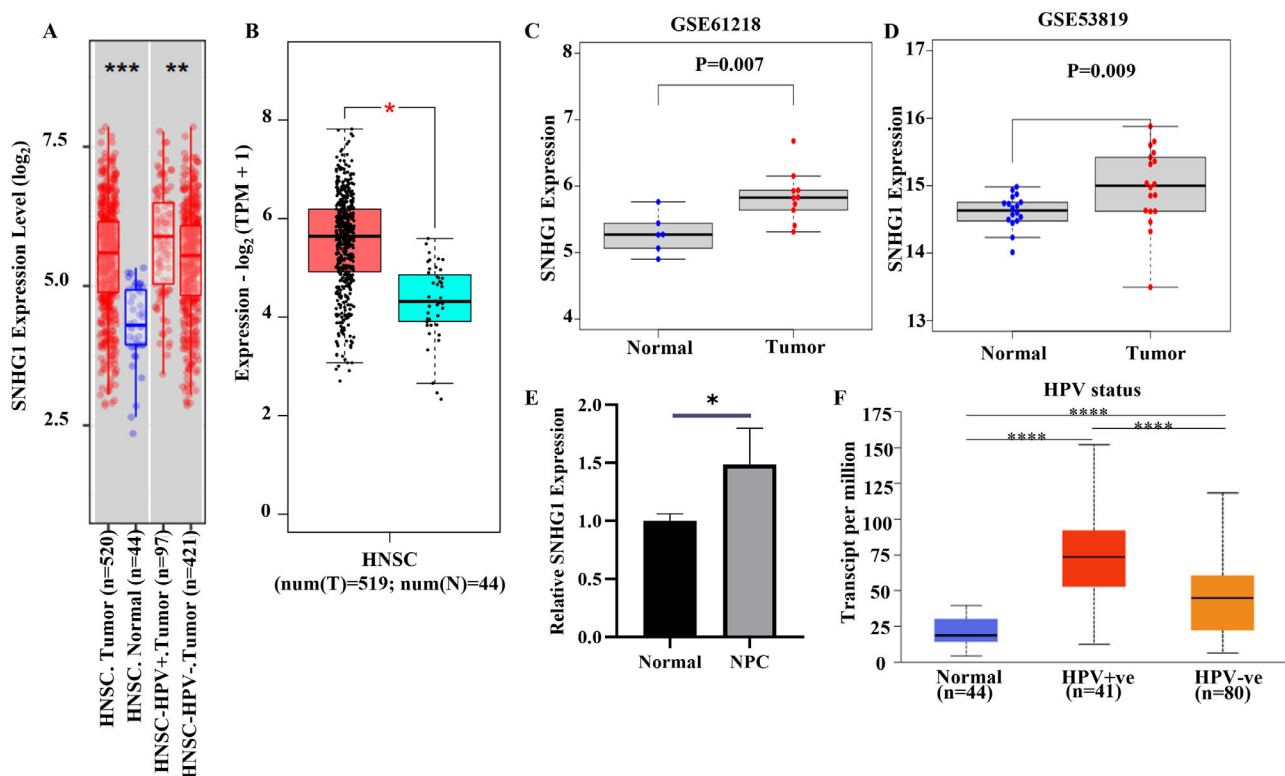


Figure 1. Expression of SNHG1 in Head and Neck Cancer (HNSC) and nasopharyngeal carcinoma (NPC). A, B) Analyzed the expression of SNHG1 in HNSC based on the TIMER 2.0 (Tumor Immune Estimation Resource 2.0) and GEPIA (Gene Expression Profiling Interactive Analysis 2) databases. C, D) Analyzed the expression of SNHG1 in NPC based on the GSE61218 and GSE53819 datasets. E) The transcriptional level of SNHG1 in 4 pairs of fresh NPC and normal (non-cancerous) samples were detected by RT-qPCR. F) Analyzed the expression of SNHG1 in HNSC-HPV+, HPV-, and normal tissues based on the UALCAN (University of Alabama at Birmingham Cancer Data Analysis Portal) database. Note: * $p < 0.05$, ** $p < 0.01$, *** $p < 0.0001$, **** $p < 0.00001$

analysis results of the GEO database. We performed a correlation analysis between the expression level of SNHG1 and patient clinical characteristics in HNSC via the UALCAN database. The expression of SNHG1 was upregulated significantly when HPV+ve vs. HPV-ve ($p < 0.05$, Figure 1F). Results of other clinical characteristics were shown in the supplementary materials (Supplementary Figure S2).

Diagnostic performance of SNHG1 in NPC. We carried out the ROC analysis based on GSE61218. SNHG1 has an AUC of 0.88, sensitivity of 0.8, and specificity of 0.8, 95% CI: 0.692–1 ($p < 0.05$, Figure 2A). As for GSE53819, the AUC of SNHG1 for NPC diagnostic performance is 0.758, with a sensitivity of 1 and specificity of 0.5, 95% CI: 0.591–0.926 ($p < 0.05$, Figure 2B). The AUCs from both datasets could indicate that SNHG1 has a good diagnostic performance for NPC.

Correlation between SNHG1 and T lymphocytes. We explored the correlation between SNHG1 and T immune cells (CD4+/CD8+) in HNSC (Figure 3). SNHG1 was positively correlated with T cell CD4+ memory activated, T cell CD4+ Th1 and T cell CD4+ Th2, negatively correlated with T cell CD4+ central memory and T cell CD4+ memory resting both in HNSC and HNSC-HPV+. The results showed that SNHG1 was significantly positively correlated with T cell CD4+ Th2, negatively correlated with T cell CD4+ central memory and T cell CD4+ effector memory in HNSC-HPV-. SNHG1 was positively correlated with T cell CD8+ naive and T cell CD8+ effector memory both in HNSC and HNSC-HPV+. SNHG1 was also positively correlated with T cell

CD8+ naive in HNSC. The correlation between SNHG1 and T immune cells (CD4+/CD8+) in other cancers is shown in the supplementary data (Supplementary Figure S3).

DEGs of SNHG1 in NPC. The DEGs of SNHG1 in NPC were analyzed through the GEO database. The volcano map (Figure 4A) showed statistically significant difference in multiple genes between the two groups (SNHG1 high expression group and SNHG1 low expression group, $p < 0.05$). Red marked genes with $\log_{2}FC > 1$ and green with $\log_{2}FC < -1$. The thermal diagram (Figure 4B) and the Venn diagram (Figure 4C) showed 40 DEGs such as TSPAN19, WSCD1, ARMC3, SNTN, MORN5, AKAP14, TEK1, C6orf118, and FHOD3, which closely related to the expression of SNHG1 in NPC based on GSE61218 and GSE53819.

PPI networks. SNHG1-related DEGs from the GSE61218 dataset were input into the string database to obtain a PPI network diagram (Supplementary Figure S4). The Cytoscape results showed that TOP2A, CCNB2, DTL, PBK, NUF2, RACGAP1, TTK, RAD51AP1, NDC80, NUSAP1, and other core targets with darker colors (red) in the diagram (Figure 5A). Figures 5B–5E revealed the subnetworks (1–4) of the PPI network: subnetwork 1 is related to cell cycle, mitotic cell cycle, etc.; subnetwork 2 is related to type I interferon signaling pathways, defense against viral responses, and negative regulation of viral genome replication, etc.; subnetwork 3 is related to cell chemotaxis, immune response, and chemokine mediated signaling pathways, etc.; and subnetwork 4 is associated with Axon guidance, negative regulation of axonal extension, and negative chemotaxis.

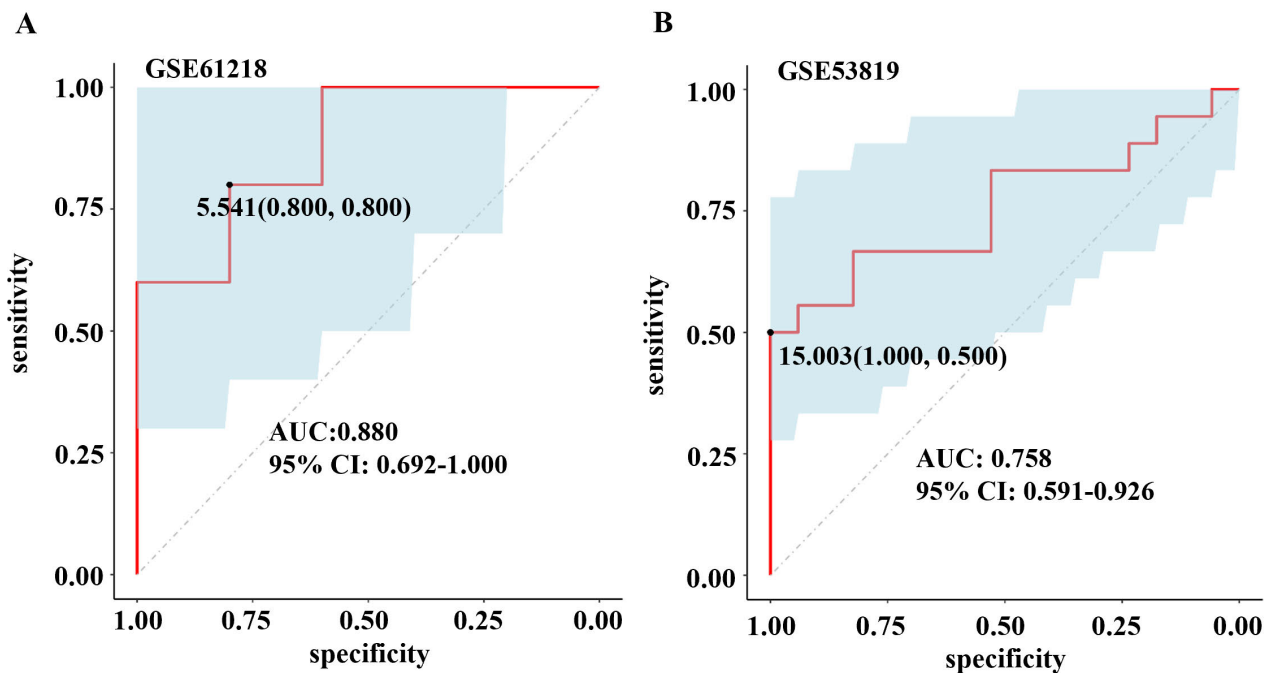


Figure 2. The receiver operating characteristic curve (ROC) of SNHG1 in NPC. ROC of SNHG1 could distinguish NPC from non-cancerous tissues (GSE61218 (A); GSE53819 (B)), the red curve is the ROC curve, and the blue shaded part represents 95% CI.

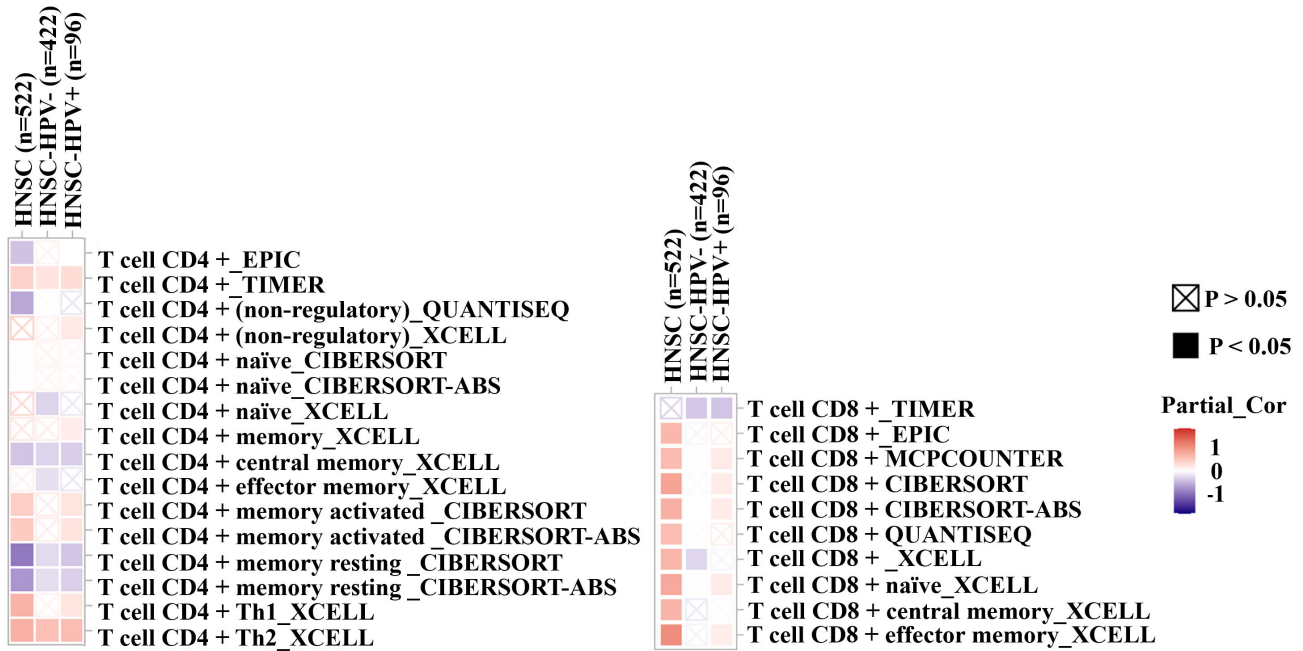


Figure 3. Correlation between SNHG1 and T lymphocytes (CD4+/CD8+) in HNSC. Note: Red indicates a positive correlation, while violet indicates a negative correlation, and the darker the color, the stronger the correlation.

The GSE53819 dataset SNHG1-related DEGs were input into the string database to obtain a PPI network diagram (Supplementary Figure S5). Results showed that S100A7, SPRR1B, PI3, KRT16, IVL, CTSG, CDSN, S100A12, KRT17, and SERPINB3 were core targets, with darker colors (red) in the diagram (Figure 6A). Figures 6B–6F show the subnetworks (1–5) of the PPI network: molecular functions such as subnetwork 1 binding to IgE and FcεRI signal pathway, sphingomyelin signal pathway, phospholipase D signal pathway, etc.; subnetwork 2 is related to biological processes such as keratinization, *Staphylococcus aureus* infection, and estrogen signaling pathways, etc.; Subnetwork 3 is related to organisms such as antimicrobial humoral reactions, keratinocyte differentiation, and defense responses to bacteria, etc.; subnetwork 4 is related to keratinization and the keratinization envelope, etc.; and subnetwork 5 is involved in the positive regulation of epidermal growth factor activated receptor activity, the negative regulation of epidermal growth factor receptor signaling pathways, and the negative regulation of epidermal growth factor receptor signaling pathways.

GO function enrichment. The GO function enrichment results of GSE61218 and GSE53819 (SNHG1 DEGs) datasets are shown in Figure 7. SNHG1 may act on NPC through BP such as epidermis development and skin development, etc.; MF such as peptidase regulator activity and endopeptidase regulator activity, etc.; CC such as collagen-containing extracellular matrix and cell-cell junction, etc.

KEGG pathway enrichment. As shown in Figure 8, the enrichment result of the GSE61218 dataset revealed that the SNHG1 targets were enriched in signal pathways such as PI3K-AKT signaling pathway, Cytokine-Cytokine receptor interaction, Regulation of actin cytoskeleton, etc. Based on the GSE53819 dataset for enrichment analysis, the result showed that SNHG1 was enriched in signal pathways such as Cytokine-Cytokine receptor interaction, Neuroactive ligand receptor interaction, and PI3K-AKT signaling pathway. It can be seen that SNHG1 is likely to promote the occurrence and development of NPC through the PI3K-AKT signaling pathway.

H&E staining pathological results. The HE staining results are shown in Figure 9. Compared with NPS, the cells in NPC tissue samples are characterized by oval or spindle shape; significant heteromorphism, large, deeply stained, or vacuolate nuclei; unbalance in nucleocytoplasmic ratio; prominent nucleoli and mitotic figures.

IHC and pathological results of the PI3K-AKT pathway. We used IHC staining to detect and analyze the expression levels of target proteins (PI3K, AKT/pAKT, EGFR, and CASP3) in the PI3K-AKT signaling pathway in 36 cases of NPS and 36 cases of NPC. We found that PI3K, AKT/pAKT, and CASP3 are mainly expressed in the cytoplasm of NPC, EGFR protein is mainly expressed in the membrane of NPC compared with NPS tissues, PI3K, AKT/pAKT, and EGFR protein are positive in NPC tissues. However, CASP3 protein is weakly positive in NPS tissues (Figure 10). The immuno-

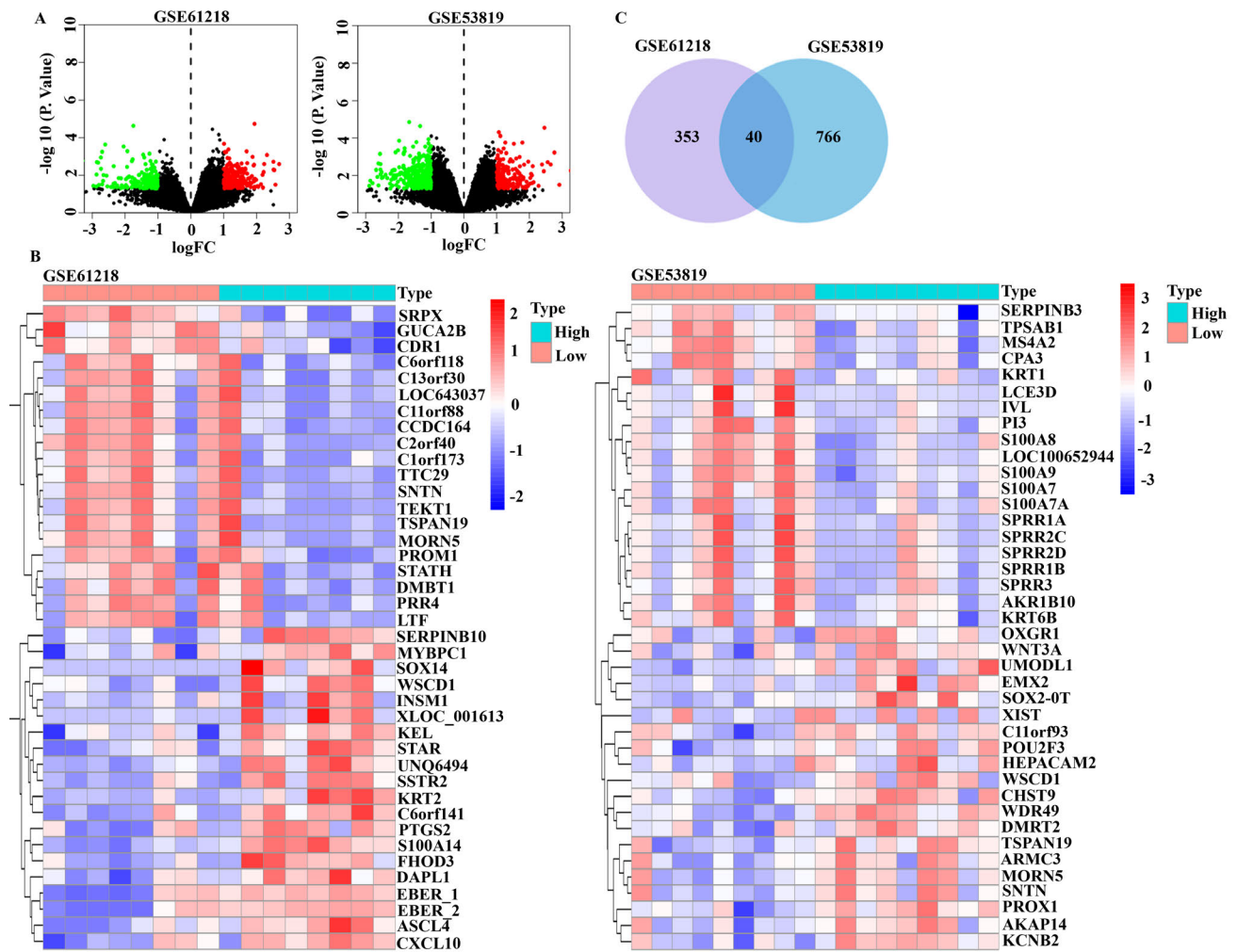


Figure 4. Differentially expressed genes (DEGs) of SNHG1 in NPC. **A**) Volcano map, where the red dot represents the $logFC > 1$ and $p < 0.05$, the green dot represents the $logFC < -1$ and $p < 0.05$, and the black dot $|logFC| < 1$ or $p > 0.05$. **B**) Heat map, in the first row of the graph, red represents samples with low SNHG1 expression, green represents samples with high SNHG1 expression. In the clustering, red represents genes positively correlated with SNHG1, and blue represents genes negatively correlated with SNHG1. **C**) Venn diagram, the violet circle represents the number of SNHG1 DEGs obtained based on the GSE61218 dataset, the blue circle represents the number of SNHG1 DEGs obtained based on the GSE53819 dataset, and the middle is the number of genes between the two datasets.

histochemical results are consistent with the bioinformatics enrichment analysis results of the GEO database.

Discussion

NPC is a highly invasive and metastatic malignant tumor that is widely prevalent in Southeast Asia and North Africa [13]. Radiotherapy combined with chemotherapy is currently the preferred treatment for NPC. However, severe adverse reactions often occur after radiotherapy. Some patients are diagnosed as mid- to late-stage, resulting in poor efficacy of radiotherapy [14, 15]. Radio-chemotherapy resistance is caused by a variety of factors, such as gene mutations, epigenetic changes, drug efflux, and other cellular and molecular mechanisms [16]. Clinically, cancer metastasis is the main

cause of cancer recurrence and mortality [17]. The main causes of metastasis in NPC can be divided into environmental, genetic, epigenetic dysregulation, and viral infection. These causes can lead to angiogenesis, cell junction destruction, cytoskeletal reorganization, protein kinase overexpression, increased mobility, escape from apoptosis, EMT, and invasion [18]. In order to improve the diagnosis and treatment of NPC, finding and establishing reliable biological markers for NPC is an important issue to be urgently resolved.

LncRNAs are non-coding RNAs with a length of more than 200 nucleotides. They play an important role in many life activities and have become a hotspot in genetic research. lncRNA SNHG1s belong to long-chain non-coding RNA, and their primary transcripts can be spliced into different

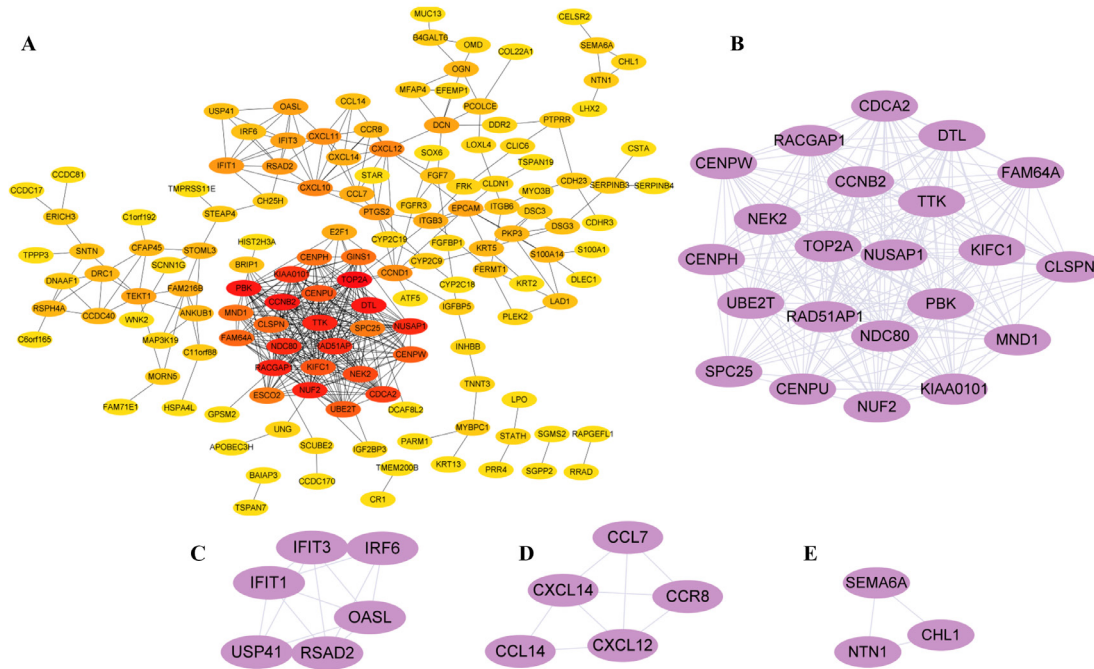


Figure 5. Protein-Protein Interaction (PPI) network of DEGs in GSE61218 dataset. A) SNHG1 related DEGs were obtained and input into the STRING database to obtain a PPI network graph. We input the result file into Cytoscape, and analyzed the core targets of the PPI network, then sorted them according to Degree. The darker the color (the redder), the more related the gene was. B–E) We obtained 4 different subnets using the Cytoscape plugin MCODE.

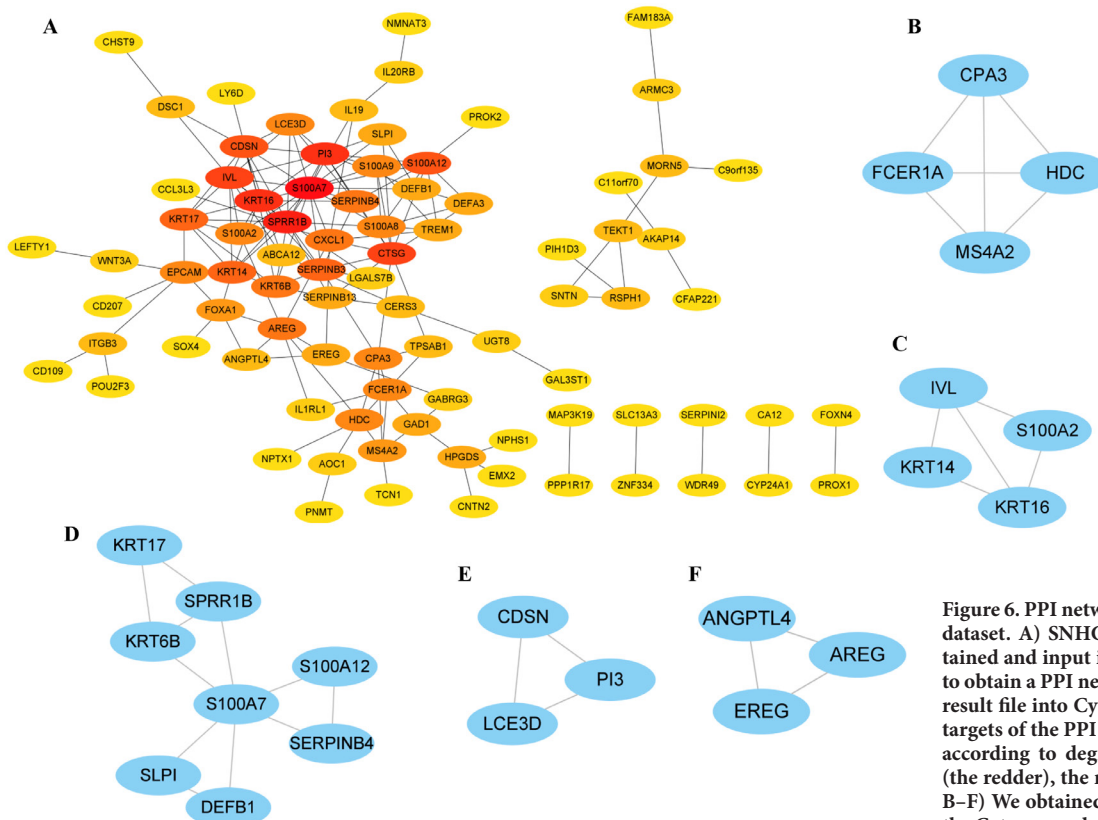


Figure 6. PPI network of DEGs in GSE53819 dataset. A) SNHG1-related DEGs were obtained and input into the STRING database to obtain a PPI network graph. We input the result file into Cytoscape, analyzed the core targets of the PPI network, and sorted them according to degree. The darker the color (the redder), the more related the gene was. B–F) We obtained 5 different subnets using the Cytoscape plugin MCODE.

exons and introns, and their introns can be further processed into snoRNA and play a role in the nucleolus [19]. Studies have shown that SNHG1s are involved in regulating the proliferation, autophagy, migration, invasion, apoptosis, and metabolic reprogramming of tumor cells in malignant tumors, and are closely related to the clinicopathological staging, distal metastasis, and prognosis of cancer patients [20–21].

SNHG1 plays a key role in the occurrence and development of cancers and has become a new carcinogen among various cancers [22–27]. SNHG1 can inhibit the apoptosis of esophageal cancer cells, and through competitive binding to miR-338, it can downregulate miR-338 expression, thereby promoting the proliferation, migration, and invasion of ESCA cells [28]. The expression level of SNHG1 in LIHC is closely related to tumor size, TNM stage, and survival time

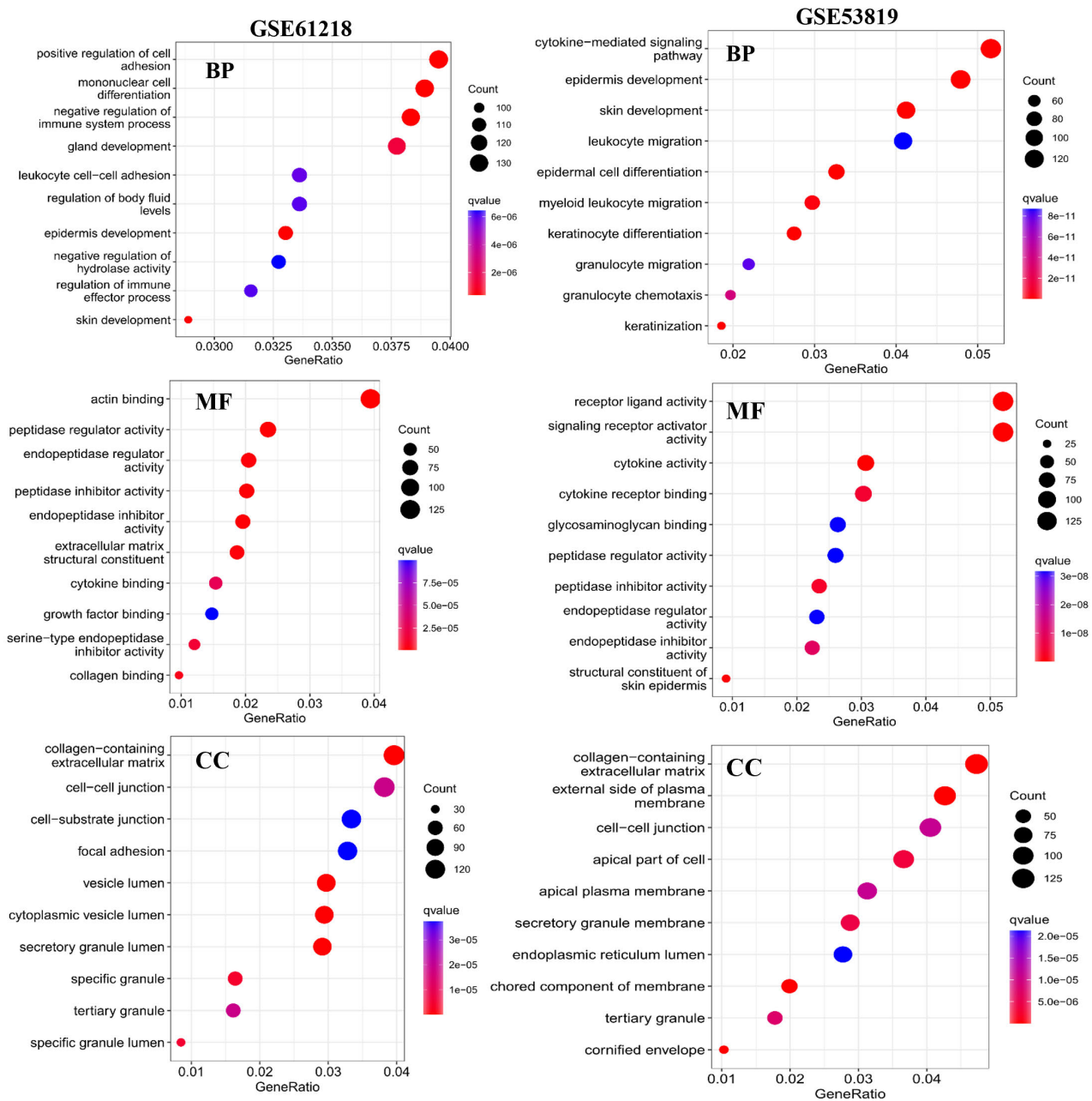


Figure 7. GO function enrichment. The SNHG1 DEGs obtained from the GSE61218 and GSE53819 datasets were subjected to GO functional enrichment analysis to obtain different biological processes (BP), molecular functions (MF), and cellular components (CC). Note: The redder the bubble color, the smaller the q value (opposite to blue), while the larger the bubble, the more genes it enriches.

[29]. SNHG1 is upregulated in COAD tissue, which is associated with reduced patient survival. After being knocked down, it significantly inhibits the growth of COAD cells [30]. SNHG1 interacts competitively with hnRNPL to inhibit the expression of protein E-cadherin, thereby activating the EMT pathway and ultimately promoting the metastasis of prostate cancer [31]. Zhou et al. found that SNHG1 could promote NPC development by inhibiting the expression of miR-424-5p [12]. However, further study is still needed to reveal the targets, pathways, and networks associated with SNHG1 in NPC.

Based on bioinformatics methods, we found that SNHG1 was significantly overexpressed in HNSC. The expression of SNHG1 is also significantly upregulated in the NPC datasets (GSE61218 and GSE53819) from the GEO database. The AUC of SNHG1 diagnostic performance is above 0.75 in both GEO datasets, indicating that SNHG1 has a high predictive ability in the diagnosis of NPC. The RT-qPCR result revealed the transcription level of SNHG1 in NPC tissues was significantly upregulated, which was consistent with the bioinformatics analysis results of the GEO database. Therefore, the upregulation of SNHG1 expression is closely related to

the occurrence and development of NPC and is a potential new diagnostic target for NPC. TME is an important factor affecting the potential of tumor biology, especially immune cell infiltration. We found the expression of SNHG1 in HNSC increased significantly with various clinical characteristics of patients, including HPV virus infection. SNHG1 was positively correlated with T cell CD4+ memory activated, T cell CD4+ Th1 and T cell CD4+ Th2, negatively correlated with T cell CD4+ central memory and T cell CD4+ memory resting in HNSC-HPV+. SNHG1 was positively correlated with T cell CD8+ naive and T cell CD8+ effector memory in HNSC-HPV+.

The results of DEGs analysis in the GSE61218 and GSE53819 datasets showed that 159 genes such as ZNF84, TGIF2, ADNP, BRX1, ATATAT1, SYCE2, and E2F5 were closely related to the expression of SNHG1 in NPC. Through KEGG enrichment analysis, these genes are significantly enriched in signal pathways such as Cytokine-Cytokine receptor interaction, PI3K-AKT signaling pathway, Chemokine signaling pathway, PI3K-AKT signaling pathway, etc. Especially, the PI3K-AKT signaling pathway was significantly enriched in both GEO datasets.

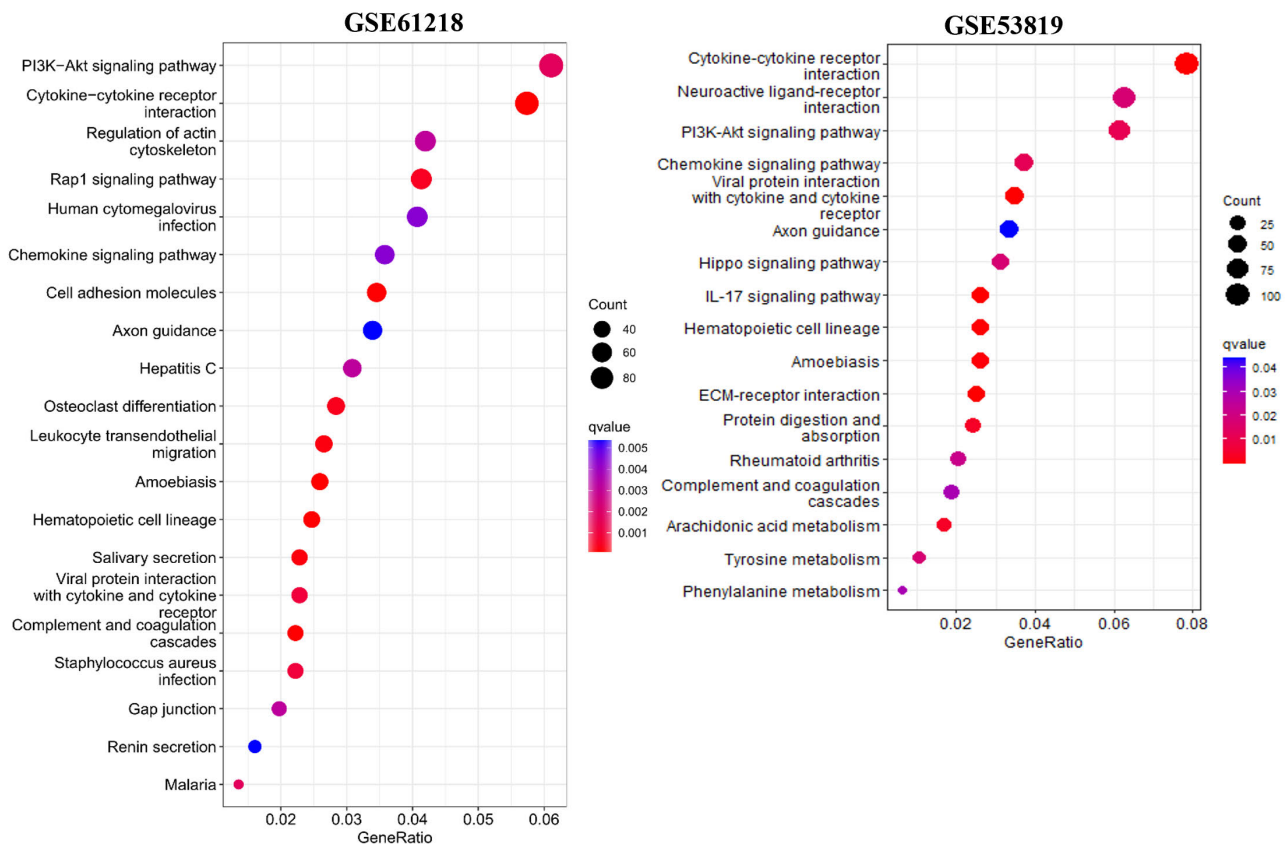


Figure 8. Enrichment of the KEGG pathway. The SNHG1 DEGs obtained from the GSE61218 and GSE53819 datasets were subjected to KEGG functional enrichment analysis to obtain different pathways. Note: The redder the bubble color in the bubble chart, the smaller the q value (opposite to blue), while the larger the bubble, the more genes enriched in this signaling pathway.

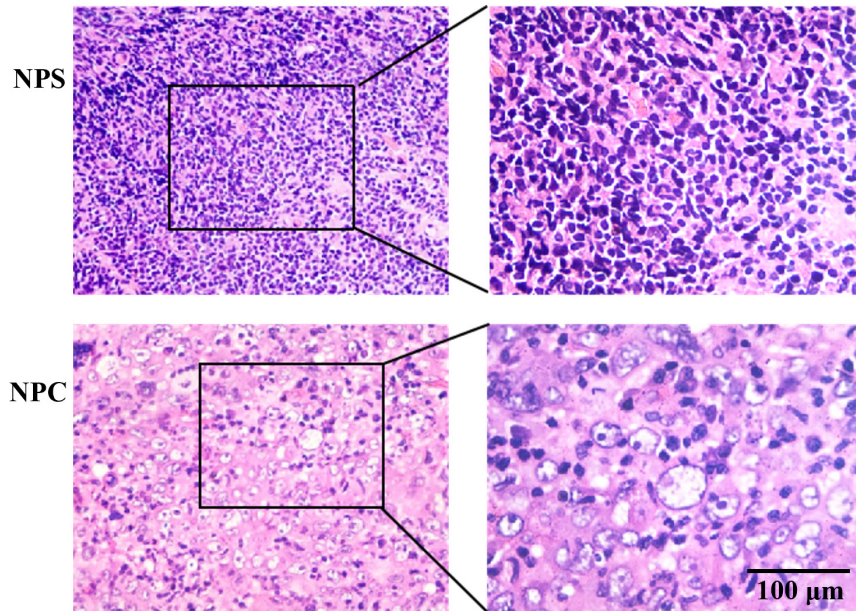


Figure 9. H&E staining results of nasopharyngitis (NPS) and NPC. Note: The left image is 20 \times , and the right image is 40 \times .

PI3K-AKT signaling pathway is an important signal transduction pathway in the occurrence and development of malignant tumors. Activation of the PI3K-AKT signaling pathway can inhibit cell apoptosis, accelerate cell growth, neovascularization, and promote the invasion and metastasis of malignant tumors [32–35]. PI3K is abnormally activated in various cancers such as NPC. It promotes the proliferation and invasion of cancer cells by phosphorylating various substrates and plays an important role in the development of cancer and the drug action mechanisms [36]. PI3K is an important growth regulator and is considered to be one of the important reasons for chemotherapy resistance in cancer treatment [37]. Activated PI3K cooperates with phosphoinositide-dependent protein kinase 1 (PDK1), phosphorylates the Ser473 and Thr308 sites of AKT, generates p-AKT to activate AKT, and is involved in regulating cancer cell proliferation, apoptosis, and angiogenesis [38–41]. SNHG1 can promote the expression of NUA1 by downregulating miR-145-5p, thereby promoting the invasiveness of NPC cells through the AKT signaling pathway [6]. The upstream targets of the PI3K-AKT signal transduction pathway include EGFR. A positive correlation between phosphorylated EGFR and phosphorylated AKT was detected in NPC patients, indicating that EGFR regulates AKT activation in NPC [42]. EGFR-specific tyrosine kinase inhibitor inhibits EGFR significantly, then inhibits the growth of NPC cells [43]. These studies demonstrate the importance of the PI3K-AKT signaling pathway in NPC.

We used immunohistochemical staining to detect and analyze the expression level of the PI3K protein in NPS and NPC tissues. We found that PI3K, AKT, and EGFR proteins were upregulated in NPC tissues compared to NPS. These

results are consistent with the KEGG enrichment analysis of GEO datasets, which confirmed that SNHG1 may act on NPC through the PI3K-AKT signal pathway.

Compared with NPS, the cells in NPC tissue samples are characterized by oval or spindle shape; significant heteromorphism, large, deeply stained, or vacuolate nuclei; unbalance in nucleocytoplasmic ratio; prominent nucleoli and mitotic figures. The heteromorphism of NPC cells is mainly due to the unlimited proliferation of cancer cells, which can cause invasion and damage to normal cells, and can also metastasize to a distant location. Generally, the greater the heteromorphism, the higher the degree of malignancy. One of the main reasons for the malignant progression of tumors is the inhibition of cell apoptosis. The main characteristics of apoptosis are phosphatidylserine externalization, mitochondrial membrane depolarization, CASP3 activation, and DNA breakage, among which CASP3 is the most important terminal-cleaving enzyme in the process of cell apoptosis [44, 45]. We used the IHC method to detect CASP3 protein in NPC tissues, and the results confirmed that the malignant progression of NPC is related to the decrease of apoptosis induced by CASP3. And CASP3 is reported to be suppressed by PI3K-AKT pathway agonists [46]. Whether SNHG1 regulates CASP3 protein in NPC remains to be further verified by more experiments.

In summary, SNHG1 is significantly overexpressed in NPC tissue and has good diagnostic performance for NPC, and its related DEGs are significantly enriched in the PI3K-AKT signaling pathway. Based on experimental results, we found that the PI3K-AKT signaling pathway has been activated. Therefore, we concluded that SNHG1 is a potential

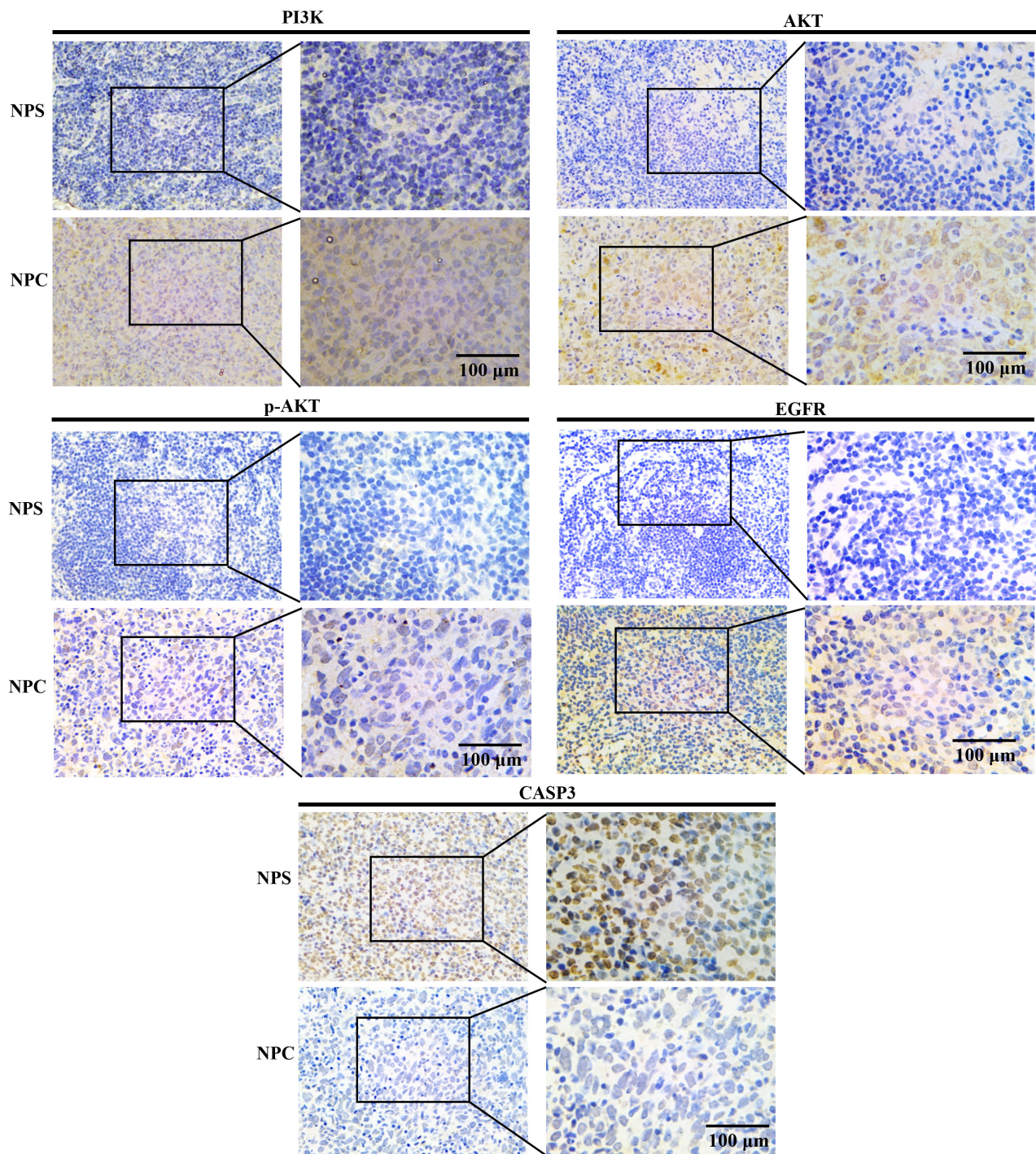


Figure 10. IHC staining results of the PI3K-AKT pathway proteins in NPS and NPC. Note: The PI3K, AKT, p-AKT, and EGFR positive expressed in NPC samples, and CASP3 positive in NPS (20× on the left and 40× on the right in each target protein group).

diagnostic marker for NPC and may act on the PI3K-AKT signaling pathway.

Supplementary information is available in the online version of the paper.

Acknowledgments: The study was financially supported by the National Natural Science Foundation of China (Grant No. [81960490]), and we would like to express our sincere gratitude to the foundation for their financial support, which greatly contributed to the completion of this research.

References

- [1] KHANFIR A, FRIKHA M, GHORBEL A, DRIRA MM, DAOUD J. Prognostic factors in metastatic nasopharyngeal carcinoma. *Cancer Radiother* 2007; 11: 461–464. <https://doi.org/10.1016/j.canrad.2007.06.006>
- [2] NGAN HL, WANG L, LO KW, LUI VWY. Genomic Landscapes of EBV-Associated Nasopharyngeal Carcinoma vs. HPV-Associated Head and Neck Cancer. *Cancers (Basel)* 2018; 10: 210. <https://doi.org/10.3390/cancers10070210>
- [3] WU J, ZHOU Q, PAN Z, WANG Y, HU L et al. Development and validation of a nomogram for predicting long-term over-all survival in nasopharyngeal carcinoma: a population-based study. *Medicine (Baltimore)* 2020; 99: e18974. <https://doi.org/10.1097/MD.00000000000018974>
- [4] JIN Y, SHI YX, CAI XY, XIA XY, CAI YC et al. Comparison of five cisplatin-based regimens frequently used as the first-line protocols in metastatic nasopharyngeal carcinoma. *J Cancer Res Clin Oncol* 2012; 138: 1717–1725. <https://doi.org/10.1007/s00432-012-1219-x>
- [5] LARBCHAROENSUB N, MAHAPROM K, JIARPINITNUN C, TRACHUN, TUBTHONGN et al. Characterization of PD-L1 and PD-1 expression and CD8+ tumor-infiltrating lymphocyte in Epstein-Barr virus-associated nasopharyngeal carcinoma. *Am J Clin Oncol* 2018; 41: 1204–1210. <https://doi.org/10.1097/COC.0000000000000449>
- [6] TANG Y, HE X. Long non-coding RNAs in nasopharyngeal carcinoma: biological functions and clinical applications. *Mol Cell Biochem* 2021; 476: 3537–3550. <https://doi.org/10.1007/s11010-021-04176-4>
- [7] LAN X, LIU X. LncRNA SNHG1 functions as a ceRNA to antagonize the effect of miR-145a-5p on the down-regulation of NUAK1 in nasopharyngeal carcinoma cell. *J Cell Mol Med* 2019; 23: 2351–2361. <https://doi.org/10.1111/jcmm.13497>
- [8] ZIMTA AA, TIGU AB, BRAICU C, STEFAN C, IONESCU C et al. An Emerging Class of Long Non-coding RNA With Oncogenic Role Arises From the snoRNA Host Genes. *Front Oncol* 2020; 10: 389. <https://doi.org/10.3389/fonc.2020.00389>
- [9] TYCOWSKI KT, SHU MD, STEITZ JA. Requirement for intron-encoded U22 small nucleolar RNA in 18S ribosomal RNA maturation. *Science* 1994; 266: 1558–1561. <https://doi.org/10.1126/science.7985025>
- [10] FREY MR, WU W, DUNN JM, MATERA AG. The U22 host gene (UHG): chromosomal localization of UHG and distribution of U22 small nucleolar RNA. *Histochem Cell Biol* 1997; 108: 365–370. <https://doi.org/10.1007/s004180050177>
- [11] SUN Y, WEI G, LUO H, WU W, SKOGERBØ G et al. The long noncoding RNA SNHG1 promotes tumor growth through regulating transcription of both local and distal genes. *Oncogene* 2017; 36: 6774–6783. <https://doi.org/10.1038/nc.2017.286>
- [12] ZHOU Z, CHEN Y. LncRNA SNHG1 promotes nasopharyngeal carcinoma development via targeting miR-424-5p. *Histol Histopathol* 2023; 38: 953–963. <https://doi.org/10.14670/HH-18-589>
- [13] WONG KCW, HUI EP, LO KW, LAM WKJ, JOHNSON D et al. Nasopharyngeal carcinoma: an evolving paradigm. *Nat Rev Clin Oncol* 2021; 18: 679–695. <https://doi.org/10.1038/s41571-021-00524-x>
- [14] LUO MS, HUANG GJ, LIU HB. Oncologic outcomes of IMRT versus CRT for nasopharyngeal carcinoma: A meta-analysis. *Medicine (Baltimore)* 2019; 98: e15951. <https://doi.org/10.1038/s41571-021-00524-x>
- [15] MCDOWELL L, CORRY J, RINGASH J, RISCHIN D. Quality of Life, Toxicity and Unmet Needs in Nasopharyngeal Cancer Survivors. *Front Oncol* 2020; 10: 930. <https://doi.org/10.3389/fonc.2020.00930>
- [16] GUAN S, WEI J, HUANG L, WU L. Chemotherapy and chemo-resistance in nasopharyngeal carcinoma. *Eur J Med Chem* 2020; 207: 112758. <https://doi.org/10.1016/j.ejmech.2020.112758>
- [17] STOLETOV K, BEATTY PH, LEWIS JD. Novel therapeutic targets for cancer metastasis. *Expert Rev Anticancer Ther* 2020; 20: 97–109. <https://doi.org/10.1080/147371402020.1718496>
- [18] PRAWIRA A, OOSTING SF, CHEN TW, DELOS SANTOS KA, SALUJA R et al. Systemic therapies for recurrent or metastatic nasopharyngeal carcinoma: a systematic review. *Br J Cancer* 2017; 117: 1743–1752. <https://doi.org/10.1038/bjc.2017.357>
- [19] TAN AQ, ZHENG YF. The Roles of SNHG Family in Osteoblast Differentiation. *Genes (Basel)* 2022; 13: 2268. <https://doi.org/10.3390/genes13122268>
- [20] CHU Q, GU X, ZHENG Q, GUO Z, SHAN D et al. Long noncoding RNA SNHG4: a novel target in human diseases. *Cancer Cell Int* 2021; 21: 583. <https://doi.org/10.1186/s12935-021-02292-1>
- [21] HAN W, SHI J, CAO J, DONG B, GUAN W. Latest Advances of Long Non-Coding RNA SNHG5 in Human Cancers. *Oncotargets Ther* 2020; 13: 6393–6403. <https://doi.org/10.2147/OTTS252750>
- [22] LI X, ZHENG H. LncRNA SNHG1 influences cell proliferation, migration, invasion, and apoptosis of non-small cell lung cancer cells via the miR-361-3p/FRAT1 axis. *Thorac Cancer* 2020; 11: 295–304. <https://doi.org/10.1111/1759-7714.13256>
- [23] CHEN Y, SHENG HG, DENG FM, CAI LL. Downregulation of the long noncoding RNA SNHG1 inhibits tumor cell migration and invasion by sponging miR-195 through targeting Cdc42 in oesophageal cancer. *Kaohsiung J Med Sci* 2021; 37: 181–191. <https://doi.org/10.1002/kjm212318>
- [24] CHEN S, GUO W, MENG M, WU D, ZHOU T et al. LncRNA SNHG1 Promotes the Progression of Pancreatic Cancer by Regulating FGFR1 Expression via Competitively Binding to miR-497. *Front Oncol* 2022; 12: 813850. <https://doi.org/10.3389/fonc.2022.813850>
- [25] ZHENG S, LI M, MIAO K, XU H. SNHG1 contributes to proliferation and invasion by regulating miR-382 in breast cancer. *Cancer Manag Res* 2019; 11: 5589–5598. <https://doi.org/10.2147/CMAR.S198624>
- [26] YE ZH, GUI DW, WANG XY, WANG J, FU JL. LncRNA SNHG1 promotes renal cell carcinoma progression through regulation of HMGA2 via sponging miR-103a. *J Clin Lab Anal* 2022; 36: e24422. <https://doi.org/10.1002/jcla.24422>

- [27] XU M, CHEN X, LIN K, ZENG K, LIU X et al. The long noncoding RNA SNHG1 regulates colorectal cancer cell growth through interactions with EZH2 and miR-154-5p. *Mol Cancer* 2018; 17: 141. <https://doi.org/10.1186/s12943-018-0894-x>
- [28] YAN Y, FAN Q, WANG L, ZHOU Y, LI J et al. LncRNA Snhg1, a non-degradable sponge for miR-338, promotes expression of proto-oncogene CST3 in primary esophageal cancer cells. *Oncotarget* 2017; 8: 35750–35760. <https://doi.org/10.18632/oncotarget.16189>
- [29] ZHANG M, WANG W, LI T, YU X, ZHU Y et al. Long noncoding RNA SNHG1 predicts a poor prognosis and promotes hepatocellular carcinoma tumorigenesis. *Biomed Pharmacother* 2016; 80: 73–79. <https://doi.org/10.1016/j.biopha.2016.02.036>
- [30] XU M, CHEN X, LIN K, ZENG K, LIU X et al. The long noncoding RNA SNHG1 regulates colorectal cancer cell growth through interactions with EZH2 and miR-154-5p. *Mol Cancer* 2018; 17: 141. <https://doi.org/10.1186/s12943-018-0894-x>
- [31] TAN X, CHEN WB, LV DJ, YANG TW, WU KH et al. LncRNA SNHG1 and RNA binding protein hnRNPL form a complex and coregulate CDH1 to boost the growth and metastasis of prostate cancer. *Cell Death Dis* 2021; 12: 138. <https://doi.org/10.1038/s41419-021-03413-4>
- [32] YANG L, WANG Q, ZHAO Q, YANG F, LIU T et al. Deglycosylated EpCAM regulates proliferation by enhancing autophagy of breast cancer cells via PI3K-AKT/mTOR pathway. *Aging (Albany NY)* 2022; 14: 316–329.
- [33] CHEN H, WANG H, YU X, ZHOU S, ZHANG Y et al. ERCC6L promotes the progression of hepatocellular carcinoma through activating PI3K-AKT and NF- κ B signaling pathway. *BMC Cancer* 2020; 20: 853. <https://doi.org/10.1186/s12885-020-07367-2>
- [34] HOU Y, CHEN K, LIAO R, LI Y, YANG H et al. LINC01419-mediated epigenetic silencing of ZIC1 promotes metastasis in hepatocellular carcinoma through the PI3K-AKT signaling pathway. *Lab Invest* 2021; 101: 570–587. <https://doi.org/10.1038/s41374-021-00539-z>
- [35] ZHANG M, LIN H, GE X, XU Y. Overproduced CPSF4 Promotes Cell Proliferation and Invasion via PI3K-AKT Signaling Pathway in Oral Squamous Cell Carcinoma. *J Oral Maxillofac Surg* 2021; 79: 1177.e1–1177.e14. <https://doi.org/10.1016/j.joms.2020.12.047>
- [36] CHOU CC, CHOU MJ, TZEN CY. PIK3CA mutation occurs in nasopharyngeal carcinoma but does not significantly influence the disease-specific survival. *Med Oncol* 2009; 26: 322–326. <https://doi.org/10.1007/s12032-008-9124-5>
- [37] LIU R, CHEN Y, LIU G, LI C, SONG Y et al. PI3K-AKT pathway as a key link modulates the multidrug resistance of cancers. *Cell Death Dis* 2020; 11: 797. <https://doi.org/10.1038/s41419-020-02998-6>
- [38] XU Y, SUI L, QIU B, YIN X, LIU J et al. ANXA4 promotes trophoblast invasion via the PI3K-AKT/eNOS pathway in preeclampsia. *Am J Physiol Cell Physiol* 2019; 316: C481–C491. <https://doi.org/10.1152/ajpcell.00404.2018>
- [39] ZHENG XY, YANG SM, ZHANG R, WANG SM, LI GB et al. Emodin-induced autophagy against cell apoptosis through the PI3K-AKT/mTOR pathway in human hepatocytes. *Drug Des Devel Ther* 2019; 13: 3171–3180. <https://doi.org/10.2147/DDDT.S204958>
- [40] LIU M, YANG P, FU D, GAO T, DENG X et al. Allicin protects against myocardial I/R by accelerating angiogenesis via the miR-19a-3p/PI3K-AKT axis. *Aging (Albany NY)* 2021; 13: 22843–22855. <https://doi.org/10.18632/aging.203578>
- [41] REVATHIDEVI S, MUNIRAJAN AK. AKT in cancer: Mediator and more. *Semin Cancer Biol* 2019; 59: 80–91. <https://doi.org/10.1016/j.semcancer.2019.06.002>
- [42] CHEUNG AKL, IP JCY, CHU ACH, CHENG Y, LEONG MML et al. PTPRG suppresses tumor growth and invasion via inhibition of AKT signaling in nasopharyngeal carcinoma. *Oncotarget* 2015; 6: 13434–13447. <https://doi.org/10.18632/oncotarget.3876>
- [43] HSU CH, GAO M, CHEN CL, YEH PY, CHENG AL. Inhibitors of epidermoid growth factor receptor suppress cell growth and enhance chemosensitivity of nasopharyngeal cancer cells in vitro. *Oncology* 2005; 68: 538–547. <https://doi.org/10.1159/000086998>
- [44] JELLINGER KA. Challenges in neuronal apoptosis. *Curr Alzheimer Res* 2006; 3: 377–391. <https://doi.org/10.2174/156720506778249434>
- [45] FEENEY B, POP C, SWARTZ P, MATTOS C, CLARK AC. Role of loop bundle hydrogen bonds in the maturation and activity of (Pro)caspase-3. *Biochemistry* 2006; 45: 13249–13263. <https://doi.org/10.1021/bi0611964>
- [46] YING J, PAN R, TANG Z, ZHU J, REN P et al. Downregulation of NCL attenuates tumor formation and growth in HeLa cells by targeting the PI3K/AKT pathway. *Cancer Med* 2022; 11: 1454–1464. <https://doi.org/10.1002/cam4.4569>